

## Nanocomposites of Reduced Graphene Oxide for Energy Storage Applications

J.G. Kim, H.K. Kim, J.P. Jegal, K.H. Kim, J.Y. Kim, S.H. Park and K.B. Kim\*

Yonsei University, 134 Shinchon-dong, Seodaemun-gu, Seoul, 120-749, South Korea

(Received 19 June; revised manuscript received 28 June 2012; published online 23 August 2012)

A well-crystallized and nano-sized Metal oxide/reduced graphene oxide composite material for lithium ion batteries has been successfully synthesized. The nano-sized metal oxide particles were evenly dispersed on the reduced graphene oxide template without any agglomeration, which allows the inherent high active surface area of individual metal oxide nano-particles in the composite. These unique structural and morphological properties of metal oxide on the highly conductive reduced graphene oxide sheets in the composite enable achieving the high specific capacity, and excellent high rate capability and stable cycling performance. An analysis of the cyclic voltammogram data revealed that a large surface charge storage contribution of the metal oxide/reduced graphene oxide nanocomposite plays an important role in achieving fast-charge/discharge.

**Keywords:** Lithium Ion Battery, Metal Oxide, Reduced Graphene Oxide, Nanocomposite.

PACS numbers: 61.05.cp, 68.37.Lp

### 1. INTRODUCTION

Reduced graphene oxide (RGO) is expected to bring about a breakthrough in many applications including electrochemical energy storage devices due to its large specific surface area, high electrical conductivity, its chemical and mechanical properties. One obvious challenge would be to utilize the 2D carbon nanostructure with regard to its large specific surface area and edge sites for the potential application in energy storage devices. RGO would be an excellent electrode materials and templates for the preparation of nanocomposites with metal oxides for electrochemical capacitor(EC) and Li ion battery applications [1, 2, 3].

Metal oxide/RGO nanocomposites are also of considerable interest for electrochemical energy storage applications owing to their unique electrical, chemical, and electrochemical properties. These excellent properties of metal oxide/RGO nanocomposites are generated from synergistic combination of RGO with metal oxide on the nanometer scale. Pseudocapacitive reaction of metal oxide is likely to occur only at the surface or a very thin surface layer of the oxide. Therefore, metal oxide/RGO nanocomposites, where metal oxide forms only on the surface of RGO on the nanometer scale with a control over particle size, particle size distribution, coating layer thickness, thickness uniformity and loading amount of metal oxide on RGOs, are expected to improve both high power and high energy properties for energy storage applications.

### 2. EXPERIMENTAL

#### 2.1 Material preparation

A  $\text{MnO}_2/\text{RGO}$  nanocomposite was first prepared by a direct redox reaction between RGO and  $\text{MnO}_4^-$  in aqueous solution. RGO nanosheets were used as a high surface area template for the selective heterogeneous nucleation and growth of  $\text{MnO}_2$ .<sup>1</sup> This  $\text{MnO}_2/\text{RGO}$  nanocomposite was then allowed to react with LiOH aqueous solution for conversion to the  $\text{LiMn}_2\text{O}_4/\text{RGO}$  nanocomposite under MAH conditions.

#### 2.2 Material Characterizations

X-Ray diffraction (XRD) patterns of the LMO/RGO nanocomposite were measured at the beamline X7B of the National Synchrotron Light Source at Brookhaven National Laboratory. The wavelength used was 0.3184 Å. The sample (5–10 mg) was loaded into a glass capillary with a diameter of 0.5 mm. Two-dimensional powder patterns were collected with an image plate detector and the powder rings were integrated using the FIT2D code. The lattice parameter was determined by a Rietveld analysis using the general structure analysis system (GSAS) program. The instrumental parameters (Thompson–Cox–Hastings profile coefficients) were derived from the fit of a  $\text{LaB}_6$  reference pattern. Transmission electron microscopy (TEM) imaging was performed on a JEOL JEM2100F TEM operated at 200 kV.

The electrochemical properties were investigated using a three-electrode electrochemical cell, with two lithium foils as counter and reference electrodes at room temperature. The working electrode was prepared by mixing 85 wt % active material ( $\text{LiMn}_2\text{O}_4/\text{RGO}$  nanocomposite,  $\text{LiMn}_2\text{O}_4$ ), 10 wt % acetylene black and 5 wt % polyvinylidene fluoride dissolved in *N*-methylpyrrolidone as a binder. The slurry mixture was coated on a titanium foil (99.7 % purity, Aldrich) and then dried at 100 °C for 24 h. Each working electrode with a  $1 \times 1 \text{ cm}^2$  area contained 1–2 mg of the dried slurry. The charge–discharge tests and cyclic voltammetry were carried out at between 3.5 and 4.5 V (*vs.* Li/Li<sup>+</sup>) using a potentiostat/galvanostat (VMP2, Princeton Applied Research). The electrolyte used was 1 M  $\text{LiPF}_6$  dissolved in a mixture of ethyl carbonate (EC) and diethyl carbonate (DEC) at a volume ratio of 1 : 1. The specific capacity was calculated based on the weight of the  $\text{LiMn}_2\text{O}_4$  in the  $\text{LiMn}_2\text{O}_4/\text{RGO}$  nanocomposite electrode. (A 1 C rate corresponds to a current rate of  $148 \text{ mA g}^{-1}$ , which in the ideal case gives complete discharge in 1 h, based on the 73 wt%  $\text{LiMn}_2\text{O}_4$  in the  $\text{LiMn}_2\text{O}_4/\text{RGO}$  nanocomposite).

\* [kbkim@yonsei.ac.kr](mailto:kbkim@yonsei.ac.kr)

### 3. RESULT AND DISCUSSION

Fig. 1 shows the X-ray diffraction (XRD) pattern of the  $\text{LiMn}_2\text{O}_4/\text{RGO}$  nanocomposite (73 wt. % of  $\text{LiMn}_2\text{O}_4$  in the  $\text{LiMn}_2\text{O}_4/\text{RGO}$  nanocomposite). All peaks could be indexed based on the cubic spinel  $\text{LiMn}_2\text{O}_4$  structure (space group:  $\text{Fd-}3\text{m}$ ). Rietveld refinement was performed using this structure and afforded an excellent fit, indicating the formation of well-crystallized spinel  $\text{LiMn}_2\text{O}_4$  phase on the RGO template without any impurity phase. The refined lattice constant  $a$  ( $8.2134 \pm 0.0002 \text{ \AA}$ ) was slightly smaller than that of bulk stoichiometric  $\text{LiMn}_2\text{O}_4$  ( $a \sim 8.235 \text{ \AA}$ ), which was attributed to either the slightly lithium-rich stoichiometry or the nano-size effect of the  $\text{LiMn}_2\text{O}_4$  formed on the RGO template. The (002) peak of RGO was very weak, implying that the  $\text{LiMn}_2\text{O}_4$  nanoparticles deposited on the RGO surface might prevent the restacking of the RGO sheets.

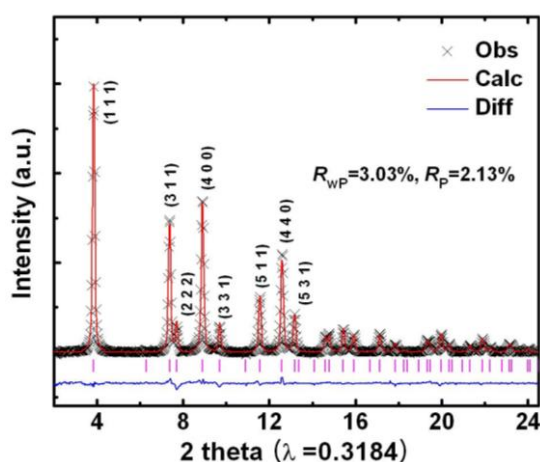


Fig. 1 – The Rietveld refinement of the spinel  $\text{LiMn}_2\text{O}_4/\text{RGO}$  nanocomposite materials

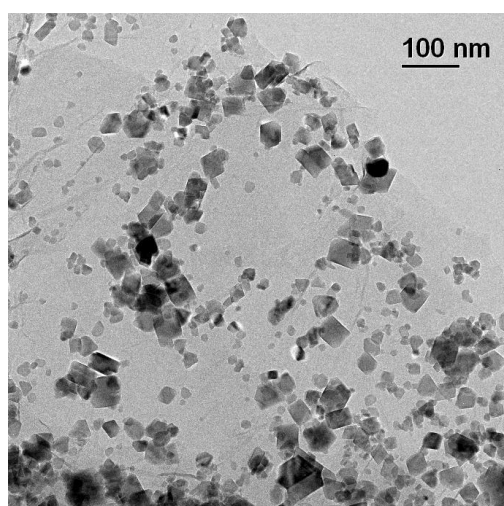


Fig. 2 – Low high-magnification TEM images of the spinel  $\text{LiMn}_2\text{O}_4/\text{RGO}$  nanocomposite materials

Transmission electron microscopy was used to investigate the morphology of the  $\text{LiMn}_2\text{O}_4/\text{RGO}$  nanocomposite material. Fig. 2 clearly shows the good dispersion and uniform coverage on the RGO nanosheets of the  $\text{LiMn}_2\text{O}_4$  nanoparticles of size 10-40 nm.

Fig. 3 shows a cyclic voltammogram (CV) of the  $\text{LiMn}_2\text{O}_4/\text{RGO}$  nanocomposite electrode in an EC/DEC electrolyte of 1M  $\text{LiPF}_6$  at increasing potential scan rate from  $1 \text{ mVs}^{-1}$  to  $10 \text{ mVs}^{-1}$ . The electrodes were fabricated by slurry casting of 85 wt. % active material ( $\text{LiMn}_2\text{O}_4/\text{RGO}$  nanocomposite), 10 wt. % acetylene black, and 5 wt. % PVDF binder dissolved in NMP solvent. The CV plot showed the typical shape of spinel  $\text{LiMn}_2\text{O}_4$  with two pairs of well-separated current peaks in the 4V region. The two pairs of current peaks in the CV suggest that the lithium ions were extracted from and inserted into the spinel structure by a two-step process, which was in good agreement with those of typical well-crystallized spinel  $\text{LiMn}_2\text{O}_4$ .

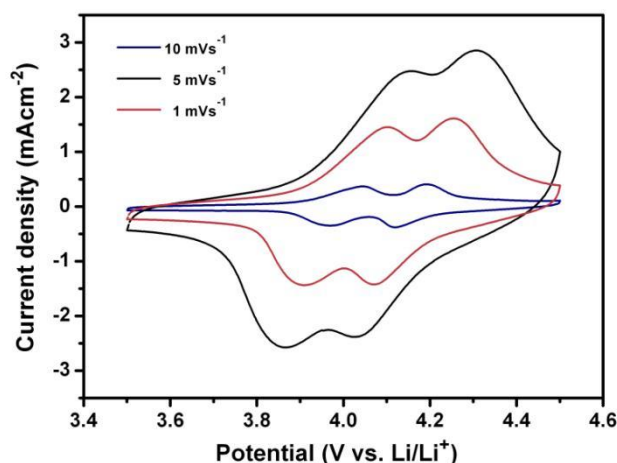


Fig. 3 – Cyclic voltammogram of the  $\text{LiMn}_2\text{O}_4/\text{RGO}$  nanocomposite electrode (CV; scan rate:  $1 \text{ mVs}^{-1} \sim 10 \text{ mVs}^{-1}$ )

The two initial current peaks of the CV at  $0.1 \text{ mVs}^{-1}$  were well distinguishable with increasing potential scan rate up to  $10 \text{ mVs}^{-1}$ , suggesting a good high rate capability for the  $\text{LiMn}_2\text{O}_4/\text{RGO}$  nanocomposite. This result is further verified by the charge/discharge curves at different C-rates. The rate performance of  $\text{LiMn}_2\text{O}_4/\text{RGO}$  was excellent, showing a capacity retention of 85 % at 50 C-rate and 74 % at 100 C-rate, compared with the specific capacity of  $137 \text{ mAhg}^{-1}$  at 1 C-rate. A comparison of the rate performance of the  $\text{LiMn}_2\text{O}_4/\text{RGO}$  nanocomposite with data from the literature further supported its excellent rate capability.

### 4. CONCLUSION

A well-crystallized and nano-sized spinel  $\text{LiMn}_2\text{O}_4/\text{RGO}$  nanocomposite cathode material for high rate lithium ion batteries was successfully synthesized by a MAH method. Combined use of microwave irradiation and graphene as a template enabled the quick synthesis of a spinel  $\text{LiMn}_2\text{O}_4/\text{RGO}$  nanocomposite material with high crystallinity and ordered structure while maintaining a well-dispersed, nano-particular shape at very low temperature. This unique structural property of the  $\text{LiMn}_2\text{O}_4$  in the nanocomposite supported a high specific capacity of  $137 \text{ mAhg}^{-1}$  at 1 C-rate and an excellent rate performance.

**ACKNOWLEDGEMENTS**

This work was supported by the National Research Laboratory Program through the National Research Foundation of Korea (NRF) grant funded by the Ministry of Education, Science and Technology (MEST) (Grant No.: 2007-0055835). The work done at BNL was sup-

ported by the Assistant Secretary for Energy Efficiency and Renewable Energy, Office of Vehicle Technologies of the U.S. Department of Energy under Contract Number DE-AC02-98CH10886.

**REFERENCES**

1. H.K. Kim, S.M. Bak, and K.B. Kim, *Electrochem. Commun.* **12**, 1768 (2010).
2. S.H. Park, S.M. Bak, K.H. Kim, J.P. Jegal, S.I. Lee, J.H. Lee, and K.B. Kim, *J. Mater. Chem.* **21**, 680 (2011).
3. S.M. Bak, K.W. Nam, C.W. Lee, K.H. Kim, H.C. Jung, X.Q. Yang and K.B. Kim, *J. Mater. Chem.* **21**, 17309 (2011).